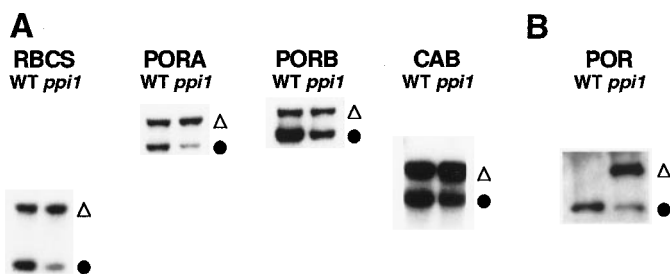


Fig. 5. Analyses of plastid protein import in the *ppi1* mutant. **(A)** In-organelle analysis of protein import into wild-type and mutant plastids isolated from 10-day-old plants. The import of four different protein precursors was investigated: RBCS, PORA, PORB, and CAB. Chloroplasts were repurified after the import reactions, and equal numbers of chloroplasts were loaded in each lane (13). **(B)** In vivo immunoblot analysis of POR protein in 5-day-old etiolated wild-type and mutant plants. Precursor proteins are indicated with open triangles; mature proteins are indicated with solid circles.



pendently, provide the simplest means of achieving the necessary pattern of expression. The fact that the translocation efficiencies of some preproteins vary between different plastid types suggests that the import machinery possesses a certain degree of specificity (18). Although our transgenic data indicate functional similarity between the two proteins (Fig. 2C), it is possible that, under normal conditions, subtle functional differences exist.

References and Notes

1. J. E. Mullet, *Annu. Rev. Plant Physiol. Plant Mol. Biol.* **39**, 475 (1988); G. K. Lamppa, G. Morelli, N.-H. Chua, *Mol. Cell. Biol.* **5**, 1370 (1985); C. Dean and R. M. Leach, *Plant Physiol.* **69**, 904 (1982); M. Viro and K. Kloppstech, *Planta* **150**, 41 (1980).
2. C. Dahlin and K. Cline, *Plant Cell* **3**, 1131 (1991); P. J. Tranel, J. Froehlich, A. Goyal, K. Keegstra, *EMBO J.* **14**, 2436 (1995).
3. H.-m. Li, K. Culligan, R. A. Dixon, J. Chory, *Plant Cell* **7**, 1599 (1995).
4. E. López-Juez, R. P. Jarvis, A. Takeuchi, A. M. Page, J. Chory, *Plant Physiol.*, in press.
5. Plants were grown on 0.5 × Murashige and Skoog medium (Gibco-BRL) containing 1.5% sucrose. Incubator temperatures were maintained at 20°C; white light fluency rates were between 200 and 300 μE m⁻² s⁻¹ (an einstein, E, is the energy of 1 mol of photons). All plants described are of the Columbia ecotype.
6. H.-m. Li and L.-J. Chen, *J. Biol. Chem.* **272**, 10968 (1997).
7. M. Seedorf, K. Waegemann, J. Soll, *Plant J.* **7**, 401 (1995); F. Kessler, G. Blobel, H. A. Patel, D. J. Schnell, *Science* **266**, 1035 (1994).
8. The close linkage of a single-locus T-DNA insertion to the mutant locus was established by analyzing the cosegregation of the kanamycin-resistant (T-DNA-associated) and pale phenotypes in the progeny of a segregating population of 68 second-generation transformants. Genomic DNA flanking the T-DNA left border was isolated with a thermal asymmetric intercalated polymerase chain reaction [Y.-G. Liu, N. Mitsukawa, T. Oosumi, R. F. Whittier, *Plant J.* **8**, 457 (1995)] and found to correspond to a completely sequenced bacterial artificial chromosome (BAC) clone. Its genomic sequence and that of a full-length expressed sequence tag (EST) enabled the delineation of the structure of the disrupted gene. Database searches were performed at the U.S. National Center for Biotechnology Information (Bethesda, MD) with the BLAST program [S. F. Altschul, W. Gish, W. Miller, E. W. Myers, D. J. Lipman, *J. Mol. Biol.* **215**, 403 (1990)]. The genomic sequence and the sequence annotation were provided by Stanford University (Stanford, CA). BAC T7123 and EST 190117T7 were obtained from the *Arabidopsis* Biological Resource Center (Columbus, OH). The amino acid sequence alignment was performed with the MegAlign program (DNASTAR, Madison, WI), using the clustal method.

9. B. Fuks and D. J. Schnell, *Plant Physiol.* **114**, 405 (1997); K. Cline and R. Henry, *Annu. Rev. Cell Dev. Biol.* **12**, 1 (1996).
10. A. Kouranov and D. J. Schnell, *J. Cell Biol.* **139**, 1677 (1997); M. Akita, E. Nielsen, K. Keegstra, *ibid.* **136**, 983 (1997); M. Seedorf and J. Soll, *FEBS Lett.* **367**, 19 (1995); D. J. Schnell, F. Kessler, G. Blobel, *Science* **266**, 1007 (1994).
11. D. Schnell et al., *Trends Cell Biol.* **7**, 303 (1997).
12. P. Jarvis, L.-J. Chen, H.-m. Li, J. Chory, data not shown.
13. The methods used during the in-organelle analysis of plastid protein import were as described [S. E. Perry, H.-m. Li, K. Keegstra, *Methods Cell Biol.* **34**, 327 (1991)].
14. The Toc33 genomic construct comprised a 6.5-kb Xba I restriction fragment of BAC T7123, which was in-

serted into the plant transformation vector pPZP221 [P. Hajdukiewicz, Z. Svab, P. Maliga, *Plant Mol. Biol.* **25**, 989 (1994)]. Overexpression constructs comprised Toc33 and Toc34 cDNA clones, which were inserted into a pPZP221-based plant expression vector that carried the cauliflower mosaic virus 35S promoter and a pea ribulose 1,5-bisphosphate carboxylase/oxygenase terminator (pCHF2) [C. Fankhauser, K. Hanson, J. Chory, unpublished data].

15. Chlorophyll was extracted with *N,N*-dimethylformamide, and its concentration was determined spectrophotometrically [R. J. Porra, W. A. Thompson, P. E. Kriedemann, *Biochim. Biophys. Acta* **975**, 384 (1989)].
16. S. Reinbothe, C. Reinbothe, N. Lebedev, K. Apel, *Plant Cell* **8**, 763 (1996).
17. C. Reinbothe, K. Apel, S. Reinbothe, *Mol. Cell. Biol.* **15**, 6206 (1995).
18. J. Wan, S. D. Blakely, D. T. Dennis, K. Ko, *J. Biol. Chem.* **271**, 31227 (1996); K. Fischer et al., *ibid.* **269**, 25754 (1994).
19. Single-letter abbreviations for the amino acid residues are as follows: A, Ala; C, Cys; D, Asp; E, Glu; F, Phe; G, Gly; H, His; I, Ile; K, Lys; L, Leu; M, Met; N, Asn; P, Pro; Q, Gln; R, Arg; S, Ser; T, Thr; V, Val; W, Trp; and Y, Tyr.
20. We thank J. Lutes for technical assistance; D. Weigel, M. Surpin, and R. Larkin for comments on the manuscript; and G. Armstrong and K. Apel (Eidgenössische Technische Hochschule, Zürich) for providing the POR antiserum. Supported by U.S. Department of Energy grant ER 13993 (J.C.), by Academia Sinica and National Science Council of Taiwan grant NSC 87-2312-B-001-018 (H.-m.L.), and by Human Frontier Science Program fellowships (P.J. and C.F.). J.C. is an associate investigator of the Howard Hughes Medical Institute.

16 June 1998; accepted 21 August 1998

Hepatitis C Viral Dynamics in Vivo and the Antiviral Efficacy of Interferon-α Therapy

Avidan U. Neumann,*† Nancy P. Lam,*‡ Harel Dahari, David R. Gretch, Thelma E. Wiley, Thomas J. Layden, Alan S. Perelson

To better understand the dynamics of hepatitis C virus and the antiviral effect of interferon-α-2b (IFN), viral decline in 23 patients during therapy was analyzed with a mathematical model. The analysis indicates that the major initial effect of IFN is to block virion production or release, with blocking efficacies of 81, 95, and 96% for daily doses of 5, 10, and 15 million international units, respectively. The estimated virion half-life ($t_{1/2}$) was, on average, 2.7 hours, with pretreatment production and clearance of 10¹² virions per day. The estimated infected cell death rate exhibited large interpatient variation (corresponding $t_{1/2} = 1.7$ to 70 days), was inversely correlated with baseline viral load, and was positively correlated with alanine aminotransferase levels. Fast death rates were predictive of virus being undetectable by polymerase chain reaction at 3 months. These findings show that infection with hepatitis C virus is highly dynamic and that early monitoring of viral load can help guide therapy.

Chronic infection with hepatitis C virus (HCV) is alarmingly prevalent (2 to 15%) throughout the world; 20 to 30% of infected people may develop cirrhosis and 1 to 3% may develop liver cancer (1). Unfortunately, the current treatment with interferon (IFN) is successful in only 11 to 30% of cases (1), and the mechanism of action is not well understood (2). In other viral infections, such as human immunodeficiency virus (HIV) (3) and hepatitis B virus

(HBV) (4), analysis of viral dynamics during antiviral therapy has been helpful in understanding pathogenesis and in guiding therapy. The kinetics of HCV during IFN therapy has been described recently (5–7), but the underlying viral dynamics and the effect of IFN are not yet well understood.

In a preliminary study (6), we observed a dose-dependent acute HCV RNA decline in serum over a 1-day period after a single injec-

REPORTS

tion of IFN. However, because of the limited frequency and duration of sampling, we were able to obtain only a minimal estimate of the free virion clearance rate and the steady-state HCV production rate. Nevertheless, we hypothesized that IFN acts by blocking the production or release of virions (6) rather than by blocking de novo infection (5). In this study, mathematical analysis is coupled with very frequent sampling of serum HCV RNA during 14 days of treatment with higher daily doses of IFN. This study not only corroborates our previous hypothesis, but it allows us to estimate the absolute efficacy of IFN therapy—that is, the percentage of HCV production blocked by different doses of IFN. Furthermore, we now estimate the infected cell death rate, an important parameter for understanding HCV pathogenesis and, as we show, response to therapy. All together the analysis gives a complete understanding of HCV dynamics and IFN effect.

Twenty-three patients infected with HCV genotype 1 (8), who were not previously treated for HCV, were included in the study (9). The patients were randomly assigned one of three dose regimens: daily subcutaneous injections of 5, 10, or 15 million international units (mIU) of IFN- α -2b (Intron, Schering-Plough, Kenilworth, New Jersey) for 14 days, after which all received 5 mIU daily (10). Blood samples were collected every few hours during the first 2 days and daily for 2 weeks (11). The baseline viral load (12) (measured 7 and 14 days before treatment) was on average (\pm SD) $11 \times 10^6 \pm 18 \times 10^6$ HCV RNA copies per milliliter and was not significantly different among the different regimens.

After initiation of therapy, all patients exhibited a delay, on average 8.7 ± 2.3 hours, during which the viral load remained approximately at baseline (Fig. 1A). Thereafter, serum viral load rapidly declined (first phase), with average exponential decay slopes of 3.0 ± 0.7 , 6.1 ± 2.5 , and 5.0 ± 0.5 days $^{-1}$ for the 5-, 10-, and 15-mIU dose regimens, respectively. After 24 to 48 hours of treatment, the viral decline slowed with a relative stabilization at values $25\% \pm 9\%$, $5\% \pm 5\%$, and $5\% \pm 5\%$ of baseline for the 5-, 10-, and 15-mIU dose reg-

imens, respectively (Fig. 1A). The slopes and fraction of virus remaining at day 2 were significantly different between the 5-mIU regimen and the two other regimens ($P < 0.03$) (13), but there was no significant difference between the 10- and 15-mIU regimens. A slower (second phase) viral decline occurred between 2 and 14 days of treatment (Fig. 1B), with exponential decay slopes of 0.11 ± 0.14 , 0.16 ± 0.23 , and 0.28 ± 0.23 day $^{-1}$ for the 5-, 10-, and 15-mIU dose regimens, respectively, with no statistically significant difference between regimens ($P > 0.15$). The rapid first phase slope was not correlated with baseline viral load or baseline alanine aminotransferase (ALT) level. However, the slower second phase slope was found to be inversely correlated with baseline viral load ($R = -0.6$, $P = 0.006$) and positively correlated with baseline ALT level ($R = 0.6$, $P = 0.004$).

Why does HCV decline so rapidly the first day of treatment and then at a significantly slower rate? Why does the initial rate of decline depend on the IFN dose? To study these questions, we use a standard model of

viral infection (3, 4, 6), described by the differential equations

$$dT/dt = s - dT - (1 - \eta)\beta VT \quad (1)$$

$$dI/dt = (1 - \eta)\beta VT - \delta I \quad (2)$$

$$dV/dt = (1 - \varepsilon)pI - cV \quad (3)$$

where T is the number of target cells, I is the number of productively infected cells, and V is the viral load. Target cells are produced at rate s (14) and die with death rate constant d . Cells become infected with de novo infection rate constant β and, once infected, die with rate constant δ . Hepatitis C virions are produced by infected cells at an average rate of p virions per cell per day and are cleared with clearance rate constant c . The possible effects of IFN in this model are to reduce either the production of virions from infected cells by a fraction $(1 - \varepsilon)$ or the de novo rate of infection by a fraction $(1 - \eta)$. Before IFN therapy, $\varepsilon = \eta = 0$. Once therapy is initiated, $\varepsilon > 0$ or $\eta > 0$ or both. The possible effect of an immune response is not explicitly de-

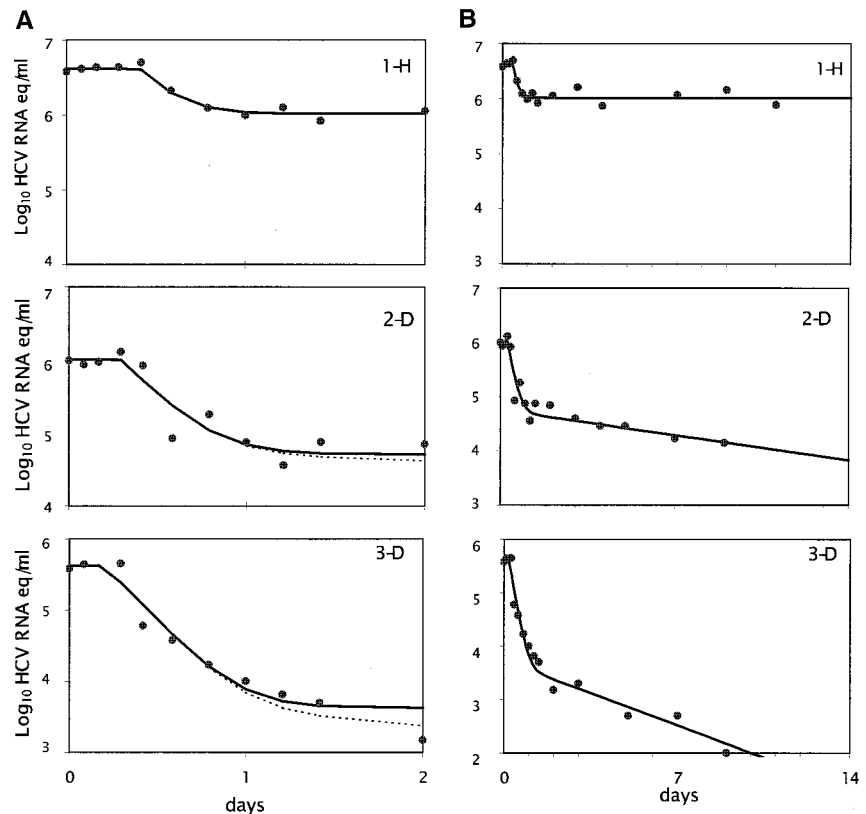


Fig. 1. HCV kinetics during the first 2 days (A) and the first 14 days (B) of IFN therapy for three representative patients receiving three different daily doses: 5 mIU (first row), 10 mIU (second row), and 15 mIU (third row). A biphasic viral decline can be observed. The first-phase slope is mainly determined by the free virion clearance rate and therapy efficacy. The second-phase slope is determined by the infected cell death rate and the efficacy and has large interpatient variation. The ratio between the viral load at day 2 and at day 0 gives a good estimate of the antiviral efficacy. On average, the slope is faster and the decrease is larger for the two higher doses (see Table 1). Solid lines in (A) are the best fit of the model to the viral load data (circles) assuming a constant level of infected cells (Eq. 4). Solid lines in (B) and dotted lines in (A) show the best fit with the full solution of the model (Eq. 5). Parameter values used are given in Table 1.

A. U. Neumann, Department of Life Sciences, Bar-Ilan University, Ramat-Gan 52900, Israel, and Santa Fe Institute, Santa Fe, NM 87501, USA. N. P. Lam, Department of Pharmacy Practice, University of Illinois, Chicago, IL 60612, USA. H. Dahari, Department of Life Sciences, Bar-Ilan University, Ramat-Gan 52900, Israel. D. R. Gretch, Hepatitis Laboratory, University of Washington, Seattle, WA 98144, USA. T. E. Wiley and T. J. Layden, Section of Digestive and Liver Diseases, Department of Medicine, University of Illinois, Chicago, IL 60612, USA. A. S. Perelson, Theoretical Division, Los Alamos National Laboratory, NM 87545, USA.

*These authors contributed equally to this work.

†To whom correspondence and questions regarding mathematical modeling and analysis should be addressed. E-mail: neumann@macs.biu.ac.il

‡To whom correspondence should be addressed. E-mail: NancyLam@uic.edu

REPORTS

scribed in this model but rather is included in the rate constants c and δ .

If IFN acts solely by blocking new HCV infections ($\eta > 0$, $\varepsilon = 0$), as postulated by others (5), or by increasing the death rate of infected cells, then HCV clearance and production would both continue at their pretreatment rate until infected cells start dying, which implies a slow first-phase decline (δ) (Fig. 2A) and not one that is 10-fold more rapid than observed during potent antiretroviral therapy for HIV (3). Moreover, blocking de novo infection would not account (Fig. 2A) for the strong dose dependence observed during the first day of therapy and for the slower decline after 2 days (Fig. 1).

If the major effect of IFN treatment is to block the production or release of virions by infected cells ($\varepsilon > 0$) in a dose-dependent manner, then upon initiation of IFN therapy a rapid, dose-dependent decline of HCV is expected (Fig. 2B). Further, if blocking is not perfect ($\varepsilon < 1$), then according to our model the viral decline will be biphasic, with the initial slope of the first phase governed by the clearance rate of free virions c and by efficacy ε . The subsequent second-phase decline is predicted to reflect the death rate of productively infected cells as well as the efficacy. The correlation of the baseline ALT level with the second-phase slope, but not with the first-phase slope, supports this model to the extent that ALT levels are an indication of the amount of hepatocyte death.

Another mode of action of IFN could be to increase the rate of virion clearance, perhaps by stimulating phagocytic cells. However, according to this hypothesis (15) the predicted pretreatment free virion half-life would vary from 0.7 day at the lowest dose to 14.3 days at the highest dose. Because the

clearance rate before treatment should be the same for the three dosages, we conclude that this hypothesis is not likely. IFN is known to have multiple effects, such as stimulating the immune system; therefore, some mechanisms of IFN action could have minor effects or become more important as treatment continues.

Based on the hypothesis that the major effect of IFN is to block viral production or release, we set $\eta = 0$ in the model and refer to

ε as the antiviral efficacy. We assume that both the viral load and the number of infected cells are in quasi-steady state (16) before therapy is initiated, with baseline at V_0 and I_0 , respectively. This assumption is supported by the fact that the maximum variation in viral load is only 3.3-fold over periods of months in untreated patients (17) and during pretreatment in our patients. If productively infected cells live much longer than 2 days, we can assume their

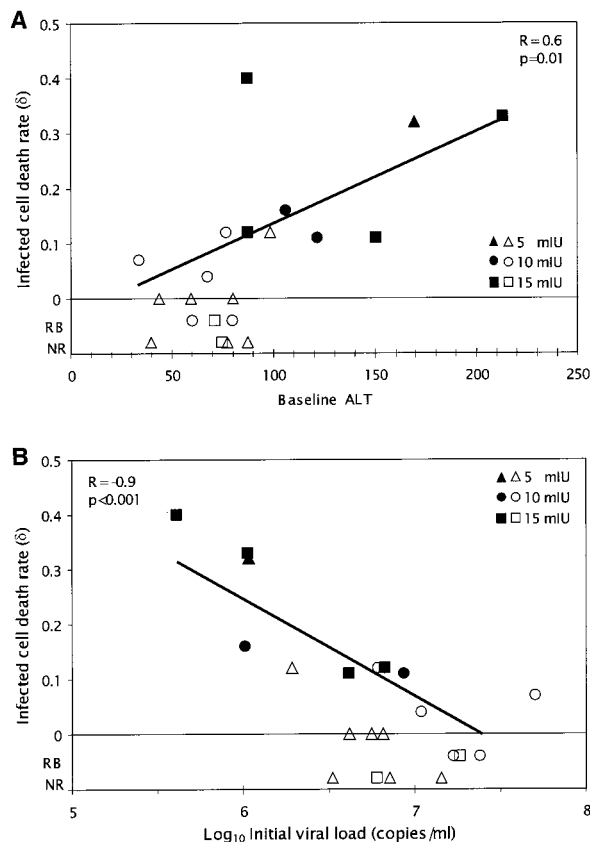
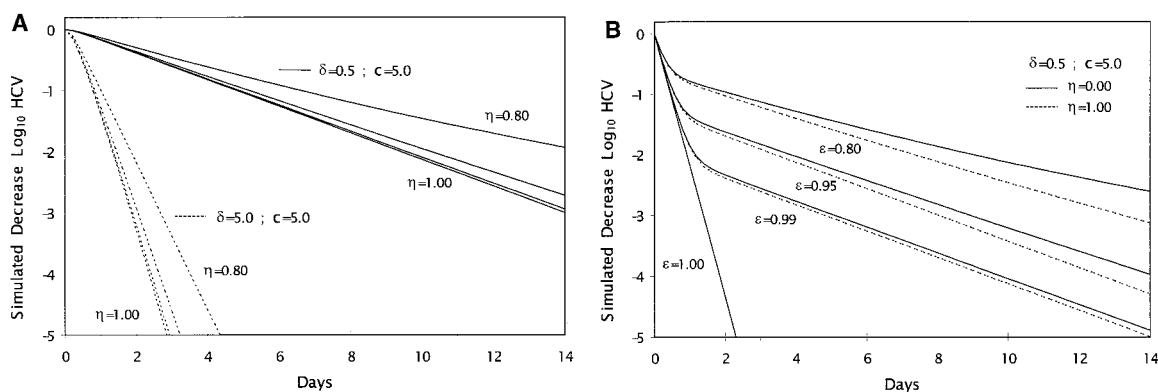


Fig. 3. Infected cell death rate (δ) is positively correlated with baseline ALT levels (A) and inversely correlated with initial viral load (B). This implies that infected cell half-life [$t_{1/2} = \ln(2)/\delta$] is longer for patients with higher initial viral loads and lower ALT levels. Patients who have undetectable HCV by PCR after 3 months of therapy (filled symbols) had significantly ($P < 0.01$) faster death rates ($\delta = 0.22 \pm 0.12 \text{ day}^{-1}$) than those who have detectable virus ($\delta = 0.05 \pm 0.05 \text{ day}^{-1}$, empty symbols). Four patients who did not respond to IFN therapy (NR) and three patients who had viral rebound (RB) have initially high HCV and low ALT levels.

Fig. 2. Predicted decrease in HCV RNA for different possible mechanisms of IFN action. The model, Eqs. 1 to 3, was solved in (A) with IFN blocking de novo infection of target cells (lines represent varying efficacy of $\eta = 0.80, 0.95, 0.99$, and 1; $\varepsilon = 0$), whereas in (B) the model was solved with IFN blocking virion production ($\varepsilon = 0.80, 0.95, 0.99$, and 1; $\eta = 0$). Assuming (solid lines) that the infected cell death rate (here, $\delta = 0.5 \text{ day}^{-1}$) is slower than the free virion clearance rate (here, $c = 5 \text{ day}^{-1}$), then only when IFN blocks HCV production can we obtain the biphasic dose-dependent kinetics observed in Fig. 1. One could assume [dashed lines in (A)] that infected cells die as fast as free virions are cleared ($\delta = 5 \text{ day}^{-1}$, $t_{1/2} = 3 \text{ hours}$ instead of $t_{1/2} = 1.4 \text{ days}$) to explain the fast decline during the first 2 days. However, even in this case, blocking infection does not explain the strong dose dependence observed during the first 2



days and the slower second-phase decline. Note that if IFN blocks production ($\varepsilon > 0$), then it could also block infection without significantly modifying the kinetics [compare dashed lines in (B), $\eta = 1$, with solid lines, $\eta = 0$]. The values of δ and c set to obtain slopes similar to those of the empirical data (see Table 1). The target cell population was held constant at a steady-state value corresponding to $T = c\delta/p\beta$, where $p = 100$ virions per milliliter per cell per day and $\beta = 3 \times 10^{-7}$ (virion per milliliter) $^{-1}$ per day, but a large range of parameter values could be used without changing these results.

REPORTS

number remains relatively constant during the first 2 days of therapy—that is, $I(t) = I_0$. The solution of Eq. 3 for the viral kinetics in the first 2 days of therapy is then

$$V(t) = V_0[1 - \varepsilon + \varepsilon \exp(-c(t - t_0))] \quad t > t_0 \quad (4)$$

where we assume that viral decay begins at time t_0 , corresponding to the delay observed in the data and possibly reflecting IFN pharmacokinetics. This solution, which has also been derived for lamivudine therapy of HBV (4), has the properties that the initial exponential decay slope is $c\varepsilon$ and that $V(t)$ approaches the constant value $(1 - \varepsilon)V_0$ after time $t \gg 1/c$. Hence, if IFN is 100% efficacious, our theory predicts that the viral load will continually decline. However, if $\varepsilon < 1$, then the viral load is predicted to stabilize at a fraction $(1 - \varepsilon)$ of the baseline.

Using nonlinear regression analysis (18), we fit the viral-load kinetics from days 0 to 2 of therapy to Eq. 4 and estimated the parameters V_0 , t_0 , c , and ε for each patient (Fig. 1A, Table 1). The virion clearance rate was, on average, $c = 6.2 \pm 1.8 \text{ days}^{-1}$, corresponding to an average half-life of $t_{1/2} = 2.7$ hours (range, 1.5 to 4.6 hours) for free serum virions. This agrees with a previous study on HCV kinetics after

liver transplantation (19). Interestingly, we found that c was not correlated with the IFN dose. The dependence of the first-phase decline slope on IFN dose is due to efficacy ε , which exhibited a strong dose dependency, with $\varepsilon = 0.81 \pm 0.06$, $\varepsilon = 0.95 \pm 0.04$, and $\varepsilon = 0.96 \pm 0.04$ for the 5-, 10-, and 15-mIU regimens, respectively. The efficacy of the 5-mIU dose is significantly ($P < 0.01$) smaller than those of the 10- and 15-mIU doses, which are comparable. On average, the fraction of serum virus remaining after 2 days of treatment is in agreement with that predicted by the model $(1 - \varepsilon)$.

For baseline viral load to be relatively constant before treatment, the extracellular viral production rate must equal the viral clearance rate (3). Thus, we estimated the production rate in each patient by the product cV_0 times a factor equal to the extracellular fluid volume (Table 1) and found an average virion production rate of 1.3×10^{12} virions per day (20). The fitted delay t_0 was, on average, 8.7 ± 2.3 hours, consistent with direct pharmacokinetic studies (21), and was independent of the IFN dose or baseline viral load (22).

Over periods longer than a few days, the death of infected cells cannot be neglected as in our approximation above. However, uninfected hepatocytes turn over slowly (23) and thus

it is reasonable to assume that T remains at its baseline value for the 2 weeks of therapy. Again assuming a pretreatment steady state, the full solution of Eqs. 2 and 3, with T constant, is

$$V(t) = V_0\{A \exp[-\lambda_1(t - t_0)] + (1 - A) \exp[-\lambda_2(t - t_0)]\} \quad t > t_0 \quad (5)$$

where

$$\lambda_{1,2} = 1/2\{(c + \delta) \pm [(c - \delta)^2 + 4(1 - \varepsilon)c\delta]^{1/2}\}$$

$$A = (\varepsilon c - \lambda_2)/(\lambda_1 - \lambda_2)$$

Next we substituted in Eq. 5 the parameters V_0 , t_0 , c , and ε , already obtained for each patient, and used nonlinear least-squares fitting (18) of the viral load data from days 0 to 14 (Fig. 1B) to estimate δ (Table 1) for each patient (24). The productively infected cell death rate was, on average, $\delta = 0.14 \pm 0.13 \text{ day}^{-1}$, with a large interpatient variation ranging from 0 (or <0.01 , the possible error in fit) to 0.4 day^{-1} , corresponding to half-lives from longer than 70 to 1.7 days.

The considerable variation in productively infected cell half-life could reflect the observed differences in cellular immunity against HCV (25), assuming that the killing of infected cells

Table 1. Fitting results. Initial viral load (VL), delay (t_0), free virion clearance rate constant (c), and therapy efficacy (ε) were estimated (18) from data obtained between day 0 and day 2 of therapy using Eq. 4, and then the infected cell death rate constant (δ) was estimated from data obtained between days 0 and 14 of therapy using Eq. 5. Total production was calculated by multiplying the clearance

rate by initial viral load and normalizing for extracellular fluid volume (20). NR, nonresponder with maximal HCV decrease of $<33\%$ and return to baseline within 14 days; RB, rebounder, viral load decreased at least 1 order of magnitude but rebounded after day 2 to within 10% of baseline; ND, no data beyond day 4, so δ could not be calculated.

Regimen	Patient	Initial VL (10^6 copies per milliliter)	Delay (hours)	Virion clearance (c)		Efficacy (ε)		Infected cell death (δ)		Production (10^9 copies per day)
				(1/day)	\pm error	Percent	\pm error	(1/day)	\pm error	
1	A	5.6	8	5.9	1.1	79	4.0%	0	0.01	495
1	B	1.9	8	6.4	1.8	75	7.0%	0.12	0.02	290
1	C	14.2	NR		NR		NR		NR	NR
1	D	7.1	NR		NR		NR		NR	NR
1	E	1.1	11	7.0	0.6	86	0.1%	0.32	0.04	125
1	F	6.5	7	5.0	0.8	89	8.0%	0	0.01	601
1	G	3.3	NR		NR		NR		NR	NR
1	H	4.1	10	6.9	0.2	75	1.0%	0	0.01	498
1: Mean	\pm SD	5.5 ± 4.1	9 ± 1.5	6.2 ± 0.8		$81 \pm 8\%$		0.09 ± 0.14		402 ± 191
2	A	6.1	7	3.6	0.2	86	0.5%	0.12	0.01	410
2	B	16.7	9	6.0	0.3	98	0.4%		RB	1409
2	C	8.6	8	6.8	0.8	96	1.0%	0.11	0.03	1089
2	D	1.0	7	5.6	0.5	95	1.0%	0.16	0.04	92
2	E	59.0	10	11.2	0.6	99.7	0.01%	0.07	0.02	12191
2	F	10.9	7	4.4	0.1	96	0.9%	0.04	0.01	965
2	G	23.8	7	4.8	0.1	92	0.8%		RB	1780
2	H	2.7	9	7.9	1.0	99.3	0.2%		ND	324
2: Mean	\pm SD	16.1 ± 18.9	8 ± 1	6.3 ± 2.4		$95 \pm 4\%$		0.1 ± 0.05		2282 ± 4045
3	A	6.7	8	3.7	0.3	99.7	0.4%	0.12	0.04	405
3	B	4.1	11	9.5	3.7	91	2.0%	0.11	0.03	761
3	C	5.8	13	5.7	0.7	98	0.5%		ND	523
3	D	0.4	5	6.0	0.8	99.0	0.2%	0.4	0.05	42
3	E	18.3	7	6.0	0.9	97.5	1.6%		RB	2136
3	F	1.1	14	5.8	0.6	90	0.3%	0.33	0.03	112
3	G	6.0	NR		NR		NR		NR	NR
3: Mean	\pm SD	6.0 ± 5.9	9.5 ± 3.5	6.1 ± 1.9		$96 \pm 4\%$		0.24 ± 0.15		663 ± 769
All: Mean	\pm SD	9.4 ± 12.4	8.7 ± 2.3	6.2 ± 1.8		—		0.14 ± 0.13		1276 ± 498

by cytotoxic T lymphocytes (CTLs) is a major contributor to the death rate of infected cells. The reported correlation between baseline ALT and anti-HCV CTL frequency (25) could explain the correlation ($R = 0.6$, $P = 0.01$) we found between baseline ALT and the death rate of infected cells (Fig. 3A). In addition, we observed, in agreement with the pretreatment steady-state solution of our model (16), that the death rate of infected cells δ is inversely correlated ($R = -0.9$; $P < 0.001$) with the initial viral load (Fig. 3B). A similar inverse correlation was found between anti-HCV CTL frequency and baseline viral load in some studies (25), but not all (26). These correlations suggest that immune control through faster killing of infected cells may have an important role in lowering HCV load. There is some trend showing faster infected cell death rates in patients receiving high IFN doses (Fig. 3), possibly due to IFN enhancement of the immune response, but these differences are not significant.

Estimates of the infected cell half-life ($t_{1/2} = \ln 2/\delta$) are important when the possibility of sustained clearance is being considered, because the virus cannot be eliminated until all infected cells die. Interestingly, we find that the infected cell death rate δ estimated during the first 2 weeks of therapy was correlated with the viral status of patients at 3 months (Fig. 3). Accordingly, none of the five patients with $\delta \leq 0.1 \text{ day}^{-1}$ had undetectable viral load [<100 RNA copies per milliliter per reverse transcriptase-polymerase chain reaction (RT-PCR)] after 3 months of therapy, and seven of nine patients who had $\delta > 0.1 \text{ day}^{-1}$ were undetectable at 3 months ($P = 0.005$, χ^2 test). This suggests that success with IFN therapy could be predicted from the early dynamics and that, if high values of δ reflect a strong pretreatment cellular immune response against HCV, CTL responses may be needed for successful IFN therapy (27).

The rate of HCV production found here is larger than the current estimates for viral production in HIV-infected individuals (3). The large viral production rate clarifies why HCV appears as a quasi-species as diverse as HIV (28) and implies that mutations that make the virus more fit under treatment could be rapidly produced. Indeed, it was found (29) that failure of IFN treatment is associated with large quasi-species diversity and high viral load, similar to the trend we found here (Fig. 3). Thus, as for HIV, initially treating HCV aggressively should be considered as a means of increasing the success of therapy.

Our results indicate that IFN doses of 10 and 15 mIU daily have significantly better early antiviral efficacy than a dose of 5 mIU daily and, based on our previous findings (6), higher efficacy than the standard dose of 3 mIU. Studies with more patients are necessary to understand the importance of this early antiviral efficacy, manifested as the drop in viral load after

2 days of therapy, as well as the rate of the second-phase decline on the long-term success of treatment. Uncovering the rapid dynamics of HCV has implications for the possible emergence of viral resistance to new therapeutic agents, such as the protease inhibitors for HCV that are currently being designed (30), for assessing the possibility of viral eradication and for managing patient treatment.

References and Notes

1. A. M. Di Bisceglie, *Lancet* **351**, 351 (1998); J. L. Brown, *ibid.*, p. 78.
2. M. Peters, *Semin. Liver Dis.* **9**, 235 (1989).
3. D. D. Ho et al., *Nature* **373**, 123 (1995); X. Wei et al., *ibid.*, p. 117; A. S. Perelson, A. U. Neumann, M. Markowitz, J. M. Leonard, D. D. Ho, *Science* **271**, 1582 (1996); A. S. Perelson et al., *Nature* **387**, 188 (1997).
4. M. A. Nowak et al., *Proc. Natl. Acad. Sci. U.S.A.* **93**, 4398 (1996).
5. S. Zeuzem et al., *Hepatology* **23**, 366 (1996); S. Zeuzem et al., *ibid.* **28**, 245 (1998).
6. N. P. Lam et al., *ibid.* **26**, 226 (1997).
7. F. C. Bekkering et al., *ibid.*, p. 1691; N. P. Lam et al., *ibid.*, p. 1692; K. Yashi et al., *J. Infect. Dis.* **177**, 1475 (1998).
8. HCV genotypes were determined by a modification of the nested PCR procedure of Okamoto et al. [*J. Gen. Virol.* **73**, 673, (1992)] and confirmed by restriction fragment length polymorphism analysis of the 5' noncoding region.
9. Standard criteria for inclusion and exclusion of patients to IFN treatment were applied. Informed consent was obtained from all patients after the nature and the possible consequences of the study were explained to them. Data from four patients who were nonresponders were not used (Table 1), because their dynamics could not be fit with the same model as the responding patients. Detailed clinical information on these patients will be given separately (N. P. Lam et al., unpublished data).
10. Six of the patients who received 10 mIU (2A to 2F) had treatment discontinued for 1 week before they continued on the 5-mIU daily regime.
11. All serum samples (collected 0, 2, 4, 7, 10, 14, 19, and 24 hours after the first injection of IFN on day 0; 5, 10, and 24 hours after the second injection on day 1; and days 2, 3, 4, 5, 7, 9, 11, 12, and 14 before IFN injection) were separated from whole blood within 2 to 4 hours of venipuncture, divided into aliquots, and stored at -70°C .
12. Viral RNA concentrations in serum were determined both by the second generation bDNA assay (Quantiplex 2.0, Chiron Corporation, Emeryville, CA) and by the quantitative multicycle RT-PCR assay (Superquant, National Genetics Institute, Los Angeles, CA). Because of the different limits of detection and ranges of linearity of the two assays, we applied different criteria for their use in the kinetic analysis of each time period. Results from the bDNA assay were used only if viral load was above the sensitivity level of 2×10^5 eq/ml [D. R. Gretch, *Hepatology* **26**, 435 (1997)] for all samples in that period. Results from the RT-PCR assay were used only if viral load was above the sensitivity level of 100 copies per milliliter [M. J. Tong et al., *Hepatology* **26**, 1640 (1997)], but not above 10^6 copies per milliliter in all samples of the period analyzed.
13. The nonparametric Wilcoxon rank sum test was used to determine statistical significance of differences in viral fraction and slopes between dosing groups. The Spearman nonparametric test was used to assess the correlation between continuous variables. Significance was established at $P < 0.03$.
14. Other terms for production of target cells—for example, logistic growth $rT(1 - T/T_{\text{max}})$ —can be used without significantly changing the results presented here.
15. Modeling an increase in virion clearance by IFN can be done by replacing in Eq. 3 the parameter c by mC' , where m is the magnitude of the increase in clearance, and setting $\eta = \varepsilon = 0$. Solving this new model under the assumption of a pretreatment steady state, $l(t) = l_0 = C'V_0/\rho$, yields a solution that is mathe-

matically equivalent to the solution presented in Eq. 4 with $(1 - \varepsilon)$ replaced by $1/m$ and c by mC' . The value of C' for each patient is then $c(1 - \varepsilon)$ and the free virion half-life is $t_{1/2} = \ln(2)/C'$, where c and ε are given in Table 1.

16. The pretreatment quasi-steady state level of infected cells, l_0 , and free virions, V_0 , are related as shown by setting $dV/dt = 0$, $dI/dt = 0$, and $\varepsilon = \eta = 0$ in Eqs. 2 and 3. This gives $l_0 = cV_0/\rho$ and $T_0 = c\delta/\rho\beta$, where T_0 is the baseline target cell level. The full steady-state solution is obtained by also setting Eq. 1 to 0, thus also giving $V_0 = sp/c\delta - d/\delta$.
17. T. T. Nguyen et al., *J. Viral Hepatitis* **3**, 75 (1996).
18. The logarithm of Eq. 4 (or Eq. 5 as appropriate) was fit to the logarithm of the viral load data by a nonlinear least-squares method using the DNLS1 subroutine from the Common Los Alamos Software Library, which is based on a finite-difference Levenberg-Marquardt algorithm. Fits were made separately to the bDNA and to the Superquant viral load data wherever possible (12), and the average of the parameter estimates was reported. Standard errors were calculated by a bootstrap method [B. Efron and R. Tibshirani, *Stat. Sci.* **1**, 54 (1986)] in which experiments were simulated 100 times.
19. T. Fukumoto et al., *Hepatology* **24**, 1351 (1996).
20. Virus production was calculated for each patient by multiplying the initial viral load by the clearance rate and by a volume factor of 13,360 ml in extracellular fluid for a person with a standard weight of 70 kg. In our previous report (6), we mistakenly used two RNA copies per virion, and thus the production rate reported there was twofold underestimated. A production rate of 10^{12} per day, although apparently high, can be explained by a production of 10 to 100 virions per cell if a large fraction of the estimated 2×10^{11} hepatocytes are infected [S. Sherlock and J. Dooley, *Diseases of the Liver and Biliary System* (Blackwell Scientific, Oxford, ed. 10, 1997)]. Further, because of fast clearance and a large fluid volume, this production leads to the steady-state viral load of about 10^7 per milliliter observed in our patients.
21. S. Khakoo et al., *Br. J. Clin. Pharmacol.*, in press.
22. In Lam et al. (6) this delay was not noticed, probably because of less frequent sampling.
23. N. Fausto, in *Hepatology: A Textbook of Liver Disease*, T. Boyer and D. Zakim, Eds. (Saunders, Philadelphia, ed. 3, 1996), pp. 32–58.
24. δ could not be estimated in three patients (see Table 1) who had a rebound in viral load after 2 days of therapy. In addition, if there is residual HCV production during therapy, as may be indicated by the few cases where a viral rebound was observed, then δ is only a minimal estimate of the cell death rate. Further, when $\delta \ll c$, as is the case in Table 1, $\lambda_1 \approx c$, $\lambda_2 \approx \varepsilon\delta$, and $A \approx \varepsilon$.
25. D. R. Nelson et al., *J. Immunol.* **158**, 1473 (1997); K. Hiroishi et al., *Hepatology* **25**, 705 (1997).
26. B. Rehmann et al., *J. Clin. Invest.* **98**, 1432 (1996); D. K. Wong et al., *J. Immunol.* **160**, 1479 (1998).
27. D. R. Nelson et al., *Hepatology* **28**, 225 (1998).
28. M. Martell et al., *J. Virol.* **66**, 3225 (1992); D. R. Gretch and S. J. Polyak, in *Hepatitis C Virus: Genetic Heterogeneity and Viral Load*, Groupe Français d'Etudes Moléculaires des Hépatites, Eds. (John Libbey Eurotext, Paris, 1997), p. 57.
29. S. J. Polyak et al., *J. Infect. Dis.* **175**, 1101 (1997); J. M. Pawlowsky et al., *J. Virol.* **72**, 2795 (1998); S. J. Polyak et al., *ibid.*, p. 4288.
30. R. De Francesco et al., *Second International Conference on Therapies for Viral Hepatitis*, Hawaii, December 1997 (abstr. 021); A. Molla et al., *ibid.* (abstr. 023).
31. We thank the patients for their participation in the study, B. Goldstein for the use of his nonlinear fitting package, and A. Talal and J. M. Pawlowsky for helpful discussions. Portions of this work were performed under the auspices of the U.S. Department of Energy. Supported by the committee for the advancement of research of Bar-Ilan University; the Santa Fe Institute; Schering Plough Corporation, Kenilworth, NJ; the Joseph P. Sullivan and Jeanne M. Sullivan Foundation; and NIH grants RR06555, A1/DK41320-2, and A139049-2.

19 May 1998; accepted 1 September 1998